miR-375 maintains normal pancreatic α- and β-cell mass

Matthew N. Poy[a,1], Jean Hausser[b], Mirko Trajkovski[a], Matthias Braun[c], Stephan Collins[c], Patrik Rorsman[c], Mihaela Zavolan[b], and Markus Stoffel[a,2]

[a]Institute of Molecular Systems Biology, Swiss Federal Institute of Technology, ETH Zurich, CH-8093 Zurich, Switzerland; [b]Swiss Institute of Bioinformatics, Biozentrum, University of Basel, 4056 Basel, Switzerland; and [c]Oxford Centre for Diabetes, Endocrinology and Metabolism, University of Oxford, Churchill Hospital, Oxford OX3 7LJ, United Kingdom

Edited by Harvey F. Lodish, Whitehead Institute for Biomedical Research, Cambridge, MA, and approved January 26, 2009 (received for review October 23, 2008)

Altered growth and development of the endocrine pancreas is a frequent cause of the hyperglycemia associated with diabetes. Here we show that microRNA-375 (*miR-375*), which is highly expressed in pancreatic islets, is required for normal glucose homeostasis. Mice lacking *miR-375* (*375KO*) are hyperglycemic, exhibit increased total pancreatic α-cell numbers, fasting and fed plasma glucagon levels, and increased gluconeogenesis and hepatic glucose output. Furthermore, pancreatic β-cell mass is decreased in *375KO* mice as a result of impaired proliferation. In contrast, pancreatic islets of obese mice (*ob*/*ob*), a model of increased β-cell mass, exhibit increased expression of *miR-375*. Genetic deletion of *miR-375* from these animals (*375*/*ob*) profoundly diminished the proliferative capacity of the endocrine pancreas and resulted in a severely diabetic state. Bioinformatic analysis of transcript data from *375KO* islets revealed that *miR-375* regulates a cluster of genes controlling cellular growth and proliferation. These data provide evidence that *miR-375* is essential for normal glucose homeostasis, α- and β-cell turnover, and adaptive β-cell expansion in response to increasing insulin demand in insulin resistance.

diabetes | glucagon | microRNA | islet | proliferation

The maintenance of β-cell mass during development and throughout life is a highly regulated process responsible for normal glucose homeostasis. Defects in the development of pancreatic islets lead to changes in islet composition, and they often result in the hyperglycemia that characterizes the diabetic state (1, 2). The dynamic adaptation of β-cell mass in adult life is influenced by various metabolic stresses, which control the balance between proliferation and apoptosis. These processes, known to be regulated at the transcriptional level, contribute to the development and maintenance of many tissues, including the pancreatic islet (3, 4). Recent studies have shown that microRNAs (miRNAs), which regulate gene expression at a posttranscriptional level, are powerful regulators of growth, differentiation, and organ function (5–7). For instance, mutant mice in which miRNAs are collectively silenced during endocrine pancreas development exhibit defects in all pancreatic lineages, including a dramatic reduction of insulin-producing β cells (8). It is estimated that ≈30% of all protein coding genes are miRNA targets. Combining target prediction with experimental analysis of miRNA expression and production of loss of function mutants is beginning to improve our understanding of the roles that miRNAs play in normal and disease states (7–12). We have previously reported that *miR-375*, the highest expressed miRNA in pancreatic islets of humans and mice, regulates insulin secretion in isolated pancreatic β cells (13). In this study we have investigated the effect of genetic ablation of *miR-375* on pancreatic islet development and function and in the etiology of type 2 diabetes.

Results

Development of Hyperglycemia in *miR-375*-Null Mice. To elucidate the role of *miR-375* in the maintenance of glucose homeostasis and the development of the pancreatic islet in vivo, we generated *miR-375*-null mice (*375KO*) by targeted deletion and homologous recombination in embryonic stem (ES) cells. The *miR-375* gene is uniquely located within an intergenic region on mouse chromosome 1, and the targeting construct was designed to eliminate the entire ≈64-bp miRNA precursor sequence (Fig. S1*A*). Heterozygous mice were crossed and the mutants were confirmed by Southern blot analysis (Fig. S1*B*). Offspring of these intercrosses revealed genotypes of expected Mendelian ratios. An analysis of *miR-375* by in situ hybridization confirmed its expression in wild-type and its absence in *375KO* pancreatic islets (Fig. S1*C*). Northern blotting also confirmed the loss of expression in other neuroendocrine tissues in which *miR-375* is expressed at low levels (Fig. S1*D*). *MiR-375* null animals are fertile and exhibit no obvious abnormalities or changes in body mass (Fig. S1*E*).

We investigated the metabolic consequences of *miR-375* ablation by measuring fed and fasted glucose and islet hormone levels. At 4 weeks of age, male *375KO* mice exhibited random hyperglycemia (Fig. 1*A*), and by 12 weeks they developed fasting hyperglycemia (89.7 mg/dL vs. 74.7 mg/dL, $P < 0.001$, *375KO* vs. wild-type, respectively). Female *375KO* mice developed random hyperglycemia by 8 weeks in the fed state. Despite the hyperglycemic state, plasma insulin levels remained unchanged in *375KO* mice compared with wild-type littermates (Fig. 1*B*). In contrast, plasma glucagon concentrations were increased in both fasted and random-fed states (Fig. 1*C*). Mutant *375KO* mice exhibit elevated glucose levels compared with wild-type controls after an i.p. glucose challenge (Fig. 1*D*). Under identical conditions, first-phase insulin release was diminished but plasma insulin levels were unchanged between 5 and 120 min after i.p. glucose administration (Fig. 1*E*). Glucose stimulation of isolated islets from *375KO* and littermate control mice was similar over a range of concentrations (Fig. 1*F*). Furthermore, no significant differences in glucose clearance were measured during an insulin tolerance test, indicating the absence of peripheral insulin resistance (Fig. 1*G*).

We have previously shown that silencing of *miR-375* increases glucose-stimulated insulin secretion in pancreatic β-cell lines and isolated primary β cells (13). To study the effect of chronic ablation of *miR-375* on insulin secretion, we therefore measured

Author contributions: M.N.P. and M.S. designed research; M.N.P., M.T., M.B., P.R., and M.S. performed research; M.N.P., J.H., S.C., P.R., M.Z., and M.S. analyzed data; and M.N.P., S.C., M.Z., and M.S. wrote the paper.

The authors declare no conflict of interest.

This article is a PNAS Direct Submission.

Freely available online through the PNAS open access option.

[1]Present address: Max Delbrück Center for Molecular Medicine, Robert Rossle Strasse 10, 13125 Berlin, Germany.

[2]To whom correspondence should be addressed. E-mail: stoffel@imsb.biol.ethz.ch.

This article contains supporting information online at www.pnas.org/cgi/content/full/0810550106/DCSupplemental.

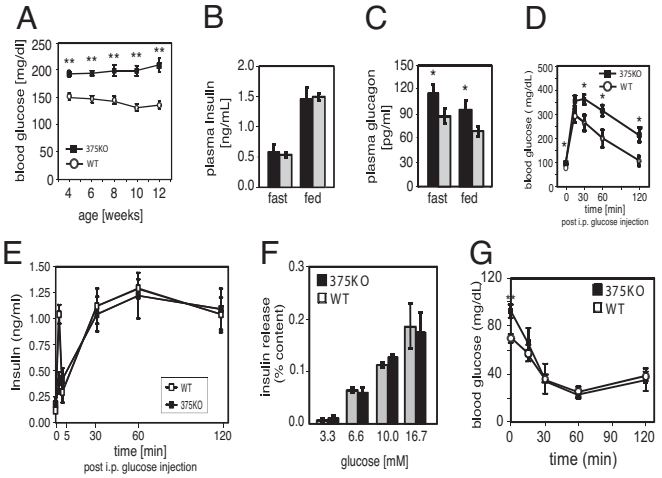

Fig. 1. *miR-375*-null mice develop diabetes. (*A*) Random-fed blood glucose levels in *375KO* (filled squares) and wild-type littermate control (open circles) male mice. (*B* and *C*) Plasma insulin and glucagon levels in 10-week-old *375KO* mice (black bars) and wild-type (gray bars) male mice. (*D*) Intraperitoneal glucose tolerance test administered to 10-week-old mice. (*E*) Plasma insulin levels during i.p. glucose tolerance test. (*F*) Insulin secretion of isolated islets in response to indicated glucose concentrations. (*G*) Insulin tolerance test of *375KO* and wild-type littermates ($n = 5$).

exocytosis in single β cells by high-resolution capacitance measurements. Exocytosis was evoked by a train of depolarizations from -70 mV to 0 mV (Fig. S2). Responses were normalized to cell size. In wild-type cells, the exocytotic responses fell from an initial value of 6 fF/pF to 1.5 fF/pF at the end of the train. The total increase in capacitance during the train was 34 ± 5 fF/pF ($n = 37$). In β cells lacking *miR-375*, the exocytotic responses fell from an initial value of 7.5 fF/pF to 3.2 fF/pF and the total response evoked by the train amounted to 55 ± 6 fF/pF ($P < 0.01$ vs. wild-type; $n = 46$) (Fig. S2 *A–C*). An identical analysis was performed on isolated α cells; however, no differences were observed between mutant and wild-type animals (Fig. S2 *D–F*). These findings extend our earlier observations implicating *miR-375* as a negative regulator of β-cell exocytosis (13). They also show that the hyperglycemia observed in *375KO* mice is not due to a deficiency in insulin secretion.

To further analyze the underlying cause for the metabolic derangements in *375KO* mice, we investigated the endocrine pancreatic cell composition of mutant and control animals. Measurement of β-cell mass of *375KO* pancreatic sections revealed a 38% and 31% decrease compared with wild-type controls at 3 and 10 weeks of age, respectively (Fig. 2*A*). Quantitative morphometric analysis of *375KO* pancreatic sections from 3-week-old mice revealed that the change in mass was due to a comparable decrease in β-cell number (Fig. 2*B*) and resulted in a 20% decrease in total endocrine cells per pancreatic area compared with control mice (Fig. 2*C*). A similar decrease was observed in β-cell number at age 10 weeks in *375KO* mice. In addition, these effects were accompanied by a 1.7-fold increase in α-cell number per pancreatic area compared with littermate controls (Fig. 2*D*). The number of δ cells was not changed in pancreata of *375KO* mice compared with controls at either age (Fig. 2*E*). No changes in total pancreatic insulin or glucagon content, or pancreatic α- and β-cell numbers, were found at postnatal day (P)14. The results observed in 3-week-old animals are the earliest detectable changes in phenotype (Fig. 2 *A–D*). The morphological analysis also revealed disrupted islet architecture with increased presence of α cells within the islet core and in the periphery (Fig. 2*F*).

To investigate if elevated plasma glucagon levels could explain

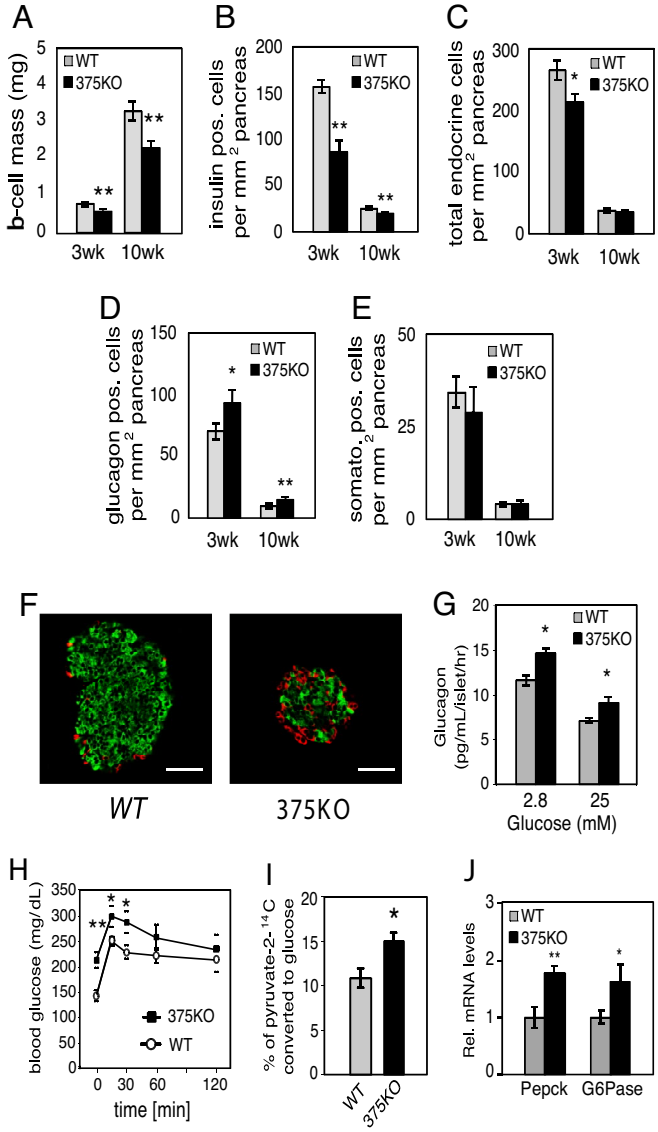

Fig. 2. Decreased β-cell mass in *375KO* pancreatic islets. (*A*) β-Cell mass in wild-type (gray bars) and *375KO* (black bars) mice is quantified and reported as mean $\pm$ SE. (*B–E*) Quantification of endocrine cell number per total pancreatic area, β-cell number (*B*), total endocrine cell number per total pancreatic area (insulin, glucagon, and somatostatin-positive cells) (*C*), α-cell number (*D*), and δ-cell number (*E*) in *375KO* (black bar) and wild-type (gray bar) male mice. (*F*) Representative sections of pancreas from 10-week-old *375KO* and wild-type male mice visualized by immunofluorescence after staining with anti-insulin (green) and anti-glucagon (red) antibodies. (Bar, 50 μm.) (*G*) Glucagon secretion measured from islets isolated from 10-week-old male *375KO* (black bars) and wild-type (gray bars) mice cultured overnight and incubated in fresh medium containing the indicated glucose concentrations. (*H*) Intraperitoneal pyruvate tolerance test was performed on random-fed 6-week-old male mice by administering a dose of sodium pyruvate (in saline) at 2 g/kg body weight. (*I*) [2-^{14}C]Pyruvate was administered by i.p. injection into random-fed 6-week-old *375KO* and wild-type (WT) mice and blood was drawn after 30 min and deproteinized, and labeled glucose in supernatant was recovered and radioactivity was measured. (*J*) Quantification of *PEPCK* and *G6Pase* mRNA expression by real-time PCR in liver from random-fed, 10-week-old *375KO* (375KO) and wild-type (WT) mice. $n = 5$–12 animals per genotype unless otherwise noted. Data are presented as means $\pm$ SE. *, $P < 0.05$; **, $P < 0.01$; ***, $P < 0.001$.

the hyperglycemia in *375KO* mice, we evaluated glucagon secretion and downstream effects in the liver. In contrast to glucose-stimulated insulin secretion, glucagon secretion was

increased in isolated pancreatic islets of *375KO* mice at both low (2.8 mM) and high (25 mM) glucose concentrations compared with wild-type littermates (Fig. 2*G*). Furthermore, pancreatic glucagon content was increased ≈3-fold compared with wild-type littermates (*375KO* vs. WT: 1.25 ± 0.28 vs. 0.41 ± 0.09 ng/mg tissue, $P \leq 0.01$, $n = 5$). Hepatic glucose production was analyzed by measuring blood glucose levels after an i.p. injection of pyruvate in random-fed mice. Significantly higher plasma glucose levels at 15 and 30 min after injection indicated that *375KO* mice have an increased ability to convert pyruvate to glucose compared with wild-type littermates (Fig. 2*H*). In addition, *375KO* mice displayed a 25% increase in the rate conversion of [2-^{14}C]pyruvate into blood glucose after i.p. injection, thereby providing further evidence that hepatic glucose production was increased in these mice (Fig. 2*I*). Similar results were obtained in fasted animals, demonstrating increased de novo synthesis of glucose by the liver in both fasted and fed conditions. Moreover, under random-fed conditions, real-time PCR analysis revealed a significant up-regulation of both phospho*enol*pyruvate carboxykinase (*PEPCK*) and glucose 6-phosphatase (*G6Pase*) in the livers of *375KO* compared with control mice, demonstrating that the hyperglucagonemia contributes to the elevated gluconeogenesis (Fig. 2*J*). Plasma and tissue levels of other neuroendocrine organs such as pituitary (growth hormone, cocaine- and amphetamine-regulated transcript), adrenal (noradrenaline, adrenaline, dopamine, corticosteroids) and intestinal (glucagon-like peptide 1, vasoactive intestinal peptide, secretin) peptides were similar in *375KO* mice and littermate controls. In addition, challenging the mice with insulin after fasting and measuring ACTH and corticosterone to test the hypothalamic–pituitary–adrenal axis revealed no abnormality between mutant and wild-type animals, indicating that loss of *miR-375* expression in the pituitary and adrenal does not contribute to the phenotype of the mutant mice. Taken together, these results show that the hyperglycemia measured in *375KO* mice is primarily caused by hyperglucagonemia resulting from an increase in pancreatic α-cell mass.

Expression of *miR-375* Is Required for Pancreatic β-Cell Compensation in Obesity. To further address the role of *miR-375* in the maintenance of β-cell mass, we measured *miR-375* expression in pancreatic islets isolated from *ob*/*ob* mice, a model for increased islet mass that is induced by severe insulin resistance (14). *miR-375* expression was increased 30% in *ob*/*ob* islets compared with wild-type controls (Fig. 3*A*). We next generated mice deficient in both *miR-375* and *leptin* (*375*/*ob*) to determine whether the increase in β-cell mass observed in *ob*/*ob* animals is dependent on *miR-375* expression. Insulin and glucagon immunostaining from 10-week old *375*/*ob* mice revealed an absence of islet hypertrophy compared with littermate control *ob*/*ob* mice (Fig. 3*B*). Pancreatic β-cell mass was decreased 71% and a similar reduction was measured in total β-cell number and total endocrine cell number per pancreatic area in *375*/*ob* animals compared with *ob*/*ob* littermates (Fig. 3 *C*–*E*). The relative number of pancreatic α cells per area of pancreas was unchanged in *375*/*ob* compared with *375KO* animals (Fig. 3*F*). Consistent with *375KO* mice, an increase in α-cell mass is reflected in an increase in the α- to β-cell ratio compared with both wild-type and *ob*/*ob* littermates (Fig. 3*G*). In addition, the decrease in β-cell number in *375*/*ob* mice was accompanied by a decrease in β cells with Ki-67-positive nuclei (Fig. 3*H*). No changes were observed in *ob*/*ob* mice in which only 1 *miR-375* allele was deleted. Failure of the islet mass to compensate for the insulin resistance induced by the obesity brought about a dramatic increase in blood glucose levels starting at age 4 weeks (Fig. 3*I*). Consistent with decreased β-cell mass, plasma insulin levels were decreased 85% in *375*/*ob* animals compared with *ob*/*ob* mice (Fig. 3*J*) and plasma glucagon levels were unchanged (129.3 ± 7.5 pg/mL vs. 120.3 ± 10.1 pg/mL, *375*/*ob* vs. *ob*/*ob*, respectively, $n = 5$–8). Furthermore, hepatic glucose production in *375*/*ob* mice was elevated 1.8-fold compared with *ob*/*ob* mice (Fig. 3*K*).

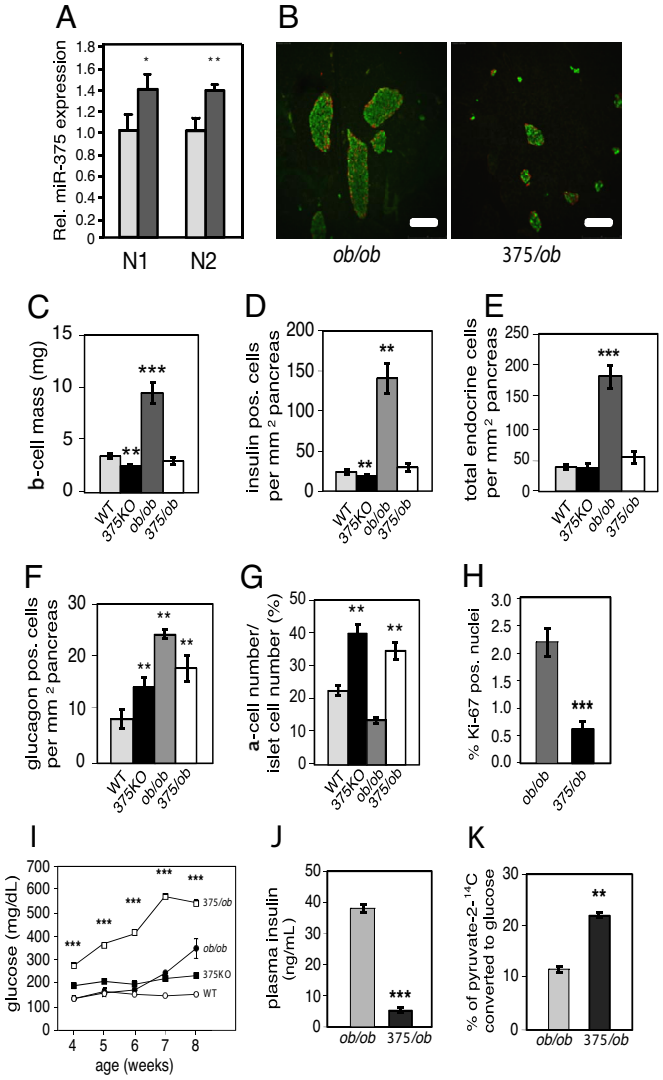

Fig. 3. Impaired β-cell proliferation in *miR-375*/*ob* double-knockout mice. (*A*) Relative *miR-375* expression in *lep*^{ob}/*lep*^{ob} (*ob*/*ob*) mice and wild-type (WT) controls measured by real-time PCR and normalized to U6 (N1) or *miR-107* (N2) expression levels. (*B*) Representative 8-μm sections of pancreas from 10-week-old *375*/*ob* (*miR-375*$^{-/-}$ *leptin*$^{-/-}$) and *ob*/*ob* mice visualized by immunofluorescence after staining with insulin (green) and glucagon (red). (Bar, 50 μm.) (*C*) β-Cell mass in 10-week-old WT (gray bar), *375KO* (black bar), *ob*/*ob* (dark gray bar), and *375*/*ob* (open bar) mice is quantified and reported as mean ± SE. (*D*–*F*) Quantification of β-cell number (insulin-positive cells), total endocrine cell number (insulin, glucagon, and somatostatin-positive cells) and α-cell number (glucagon-positive cells) per total pancreatic area in wild-type (gray bars), *375KO* (black bars), *ob*/*ob* (dark gray bars), and *375*/*ob* (open bars) 10-week-old mice. (*G*) Ratio of α-cell number to islet cell number in wild-type (gray bar), *375KO* (black bar), *ob*/*ob* (dark gray bar), and *375*/*ob* (open bar) 10-week-old mice. (*H*) Quantification of percentage of Ki-67 insulin-positive nuclei within insulin-positive cells of 10-week-old *375*/*ob* (black bar) and *ob*/*ob* (gray bar) mice. $n > 30$ for each genotype. (*I*) Random-fed blood glucose levels in *375*/*ob* (open squares), *ob*/*ob* (filled circles), *375KO* (filled squares), and wild-type littermate control (WT) (open circles) mice. (*J*) Plasma insulin levels in random-fed, 10-week-old *375*/*ob* (black bar) and *ob*/*ob* (gray bar) mice. (*K*) Hepatic glucose production measured after sodium [2-^{14}C]pyruvate was administered by i.p. injection into random-fed, 10-week-old *375*/*ob* (black bar) and *ob*/*ob* (gray bar) mice. Data are presented as means ± SE. $n = 4$–6 animals per genotype unless otherwise noted. *, $P < 0.05$; **, $P < 0.01$; ***, $P < 0.001$.

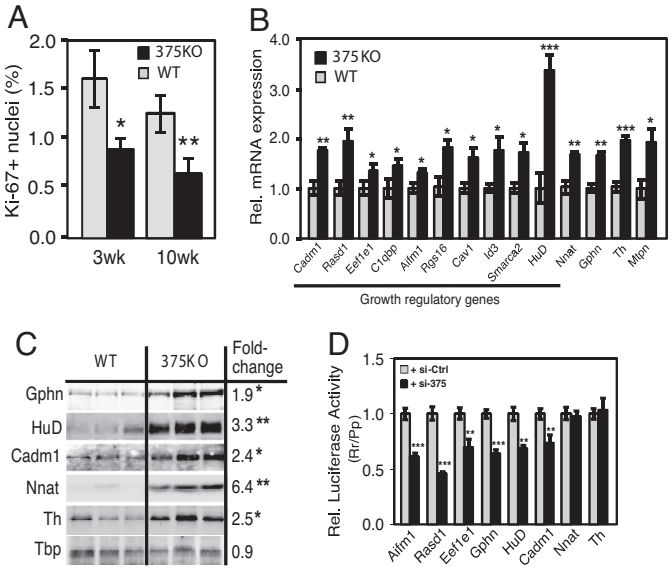

Fig. 4. Regulation of gene expression and identification of growth target genes in *375KO* islets. (*A*) Quantification of percentage of Ki-67-positive nuclei within insulin-positive cells of *375KO* (black bars) and wild-type (gray bars) male mice. (*B*) Analysis of gene expression of putative *miR-375* targets by real-time PCR in mutant and wild-type pancreatic islets. $n = 5$ animals per genotype. (*C*) Western blot analysis of protein lysates from pancreatic islets isolated from *375KO* and wild-type (*WT*) male mice (100 islets per lane). Quantitative measurements made from densitometry are expressed as a ratio of mean values of *375KO* to wild-type mice. (*D*) Increase in intracellular concentration of *miR-375* decreases luciferase activity in HEK293 cells transfected with reporter constructs containing either full-length or partial 3′UTR sequence of putative *miR-375* target genes ($n = 6$). Values relative to luciferase activity from cells transfected with a scrambled control are shown. Data are presented as means ± SE. *, $P < 0.05$; **, $P < 0.01$; ***, $P < 0.001$.

These results, in addition to the 40% decrease in body mass and measured polydipsia and polyuria, demonstrate severe insulin-deficient diabetes in *375/ob* mice compared with *ob/ob* animals.

***miR-375* Regulates Genes in Growth-Promoting Pathways.** We next addressed whether the observed decrease in β-cell mass of *375KO* mice could be reflective of changes in the rate of proliferation. Quantification of Ki-67-positive β cells, an index for cell proliferation, revealed a significant decrease in *375KO* islets at 3 and 10 weeks of age (Fig. 4*A*). A similar result was obtained measuring BrdU incorporation in β cells of *375KO* mice. To address the molecular basis for the decrease in pancreatic β-cell mass observed in the *375KO* animals, we performed gene expression analysis by using Affymetrix microarrays comparing tissues from mutant mice to wild-type littermates. Four tissues expressing different levels of *miR-375* were selected: pancreatic islets, pituitary, adrenal, and colon. Previous studies have established that miRNAs can negatively regulate the mRNA level of their direct targets (15), and that miRNA loss of function can result in the up-regulation of hundreds of genes (16). To determine the direct impact of loss of *miR-375*, we selected the most up-regulated 5% and the most down-regulated 5% of transcripts (see *SI Methods*). Each dataset thus contained 801 of the 16,301 Refseq transcripts measured by the array. We then determined the number of occurrences of the *miR-375* recognition motif GAACAAA (corresponding to nucleotides 1–7 from the 5′ end of the miRNA) in the 3′UTRs of these transcripts. When measuring gene expression from pancreatic islets of *375KO* mice compared with wild-type littermates, we counted 138 occurrences of the *miR-375* motif in the dataset of up-regulated transcripts, and 49 occurrences in the dataset of down-regulated transcripts (Fig. S3*A*). Compared with random motifs with similar frequency across the 3′UTRs of all transcripts monitored by the array (represented in the graph by a blue box plot), the 138 up-regulated transcripts represent a 1.9-fold enrichment ($P = 0.001$), whereas the 49 down-regulated transcripts represent a 1.9-fold depletion ($P = 0.002$). These results demonstrate that genetic ablation of *miR-375* in the pancreatic islet resulted in the up-regulation of direct targets of this miRNA. To further illustrate the impact of *miR-375* on islet mRNA levels, we determined the distribution of expression changes of transcripts that do include a *miR-375* motif in their 3′UTR and transcripts that do not. Transcripts that carry a *miR-375* motif are up-regulated compared with transcripts that do not ($P = 2.1 \times 10^{-24}$ in the Wilcoxon rank-sum test), and the up-regulation is even stronger for transcripts containing evolutionarily selected *miR-375* motifs ($P = 0.005$) (Fig. S3*E*). A similar analysis of gene expression in the pituitary of *375KO* mice compared with wild-type littermates revealed a significant number of up-regulated motif-containing transcripts (Fig. S3*C*). By contrast, the genes up-regulated in the adrenal and colon data sets were not enriched for the *miR-375* motif (Fig. S3 *B* and *D*). There are 2 possible explanations for this discrepancy: either the magnitude of the response from direct targets of *miR-375* depends on the endogenous expression level of the miRNA, or *miR-375* expression is limited to specific subpopulations of cells in the adrenal gland and colon. In situ hybridization using an *miR-375*-specific probe on pituitary tissue sections revealed *miR-375* to be present in both the anterior and posterior pituitary, whereas its expression within the adrenal gland appears to be limited to the medulla and the zona glomerulosa of the cortex (Fig. S4). It is not known whether *miR-375* is expressed in a specific cell type of the colon because probed tissue sections revealed no specific signal.

Several genes within the set of up-regulated transcripts of *miR-375*-null islets have been documented to negatively regulate cellular growth and were thus evaluated for direct regulation by *miR-375*. Selection of transcripts that contained a *miR-375* recognition motif resulted in 381 putative direct targets of *miR-375*. Real-time PCR analysis confirmed 10 of these genes, including caveolin1 (*Cav1*), inhibitor of DNA binding 3 (*Id3*), *Smarca2*, Ras-dexamethasone-induced-1 (*Rasd1*), regulator of G protein signaling 16 (*Rgs16*), eukaryotic elongation factor 1 epsilon 1 (*Eef1e1*), apoptosis-inducing factor, mitochondrion-associated 1 (*Aifm1*), cell adhesion molecule 1 (*Cadm1*), HuD antigen (*HuD*), and complement component 1 q subcomponent binding protein (*C1qbp*) were up-regulated in *375KO* islets (Fig. 4*B*). Increased expression of 3 additional genes, including cell adhesion molecule 1 (*Cadm1*), gephyrin (*Gphn*), and myotrophin (*Mtpn*), a previously validated target of *miR-375* (13), was confirmed in *375KO* islets by real-time PCR and Western blotting (Fig. 4 *B* and *C*). Furthermore, measurement of luciferase activity from HEK293 cells transfected with plasmid constructs containing a portion of or the entire 3′UTR of *Aifm1*, *Rasd1*, *Eef1e1*, *Gphn*, *HuD*, and *Cadm1* showed reduced expression of all these constructs in the presence of *miR-375* (Fig. 4*D*). These results suggest that Cav1, Id3, Smarca2, Aifm1, Rasd1, Rgs16, Eef1e1, C1qbp, HuD, and Cadm1, all of which have been shown to participate in signaling mechanisms that negatively regulate cellular growth and proliferation, are direct targets of *miR-375*. Published studies have shown that these genes play a role in the p53-dependent pathway (17–19), MAP kinase signaling (20), inducing apoptosis (21–23), and inhibiting normal developmental growth processes (24, 25) or the proliferation of tumors in mice (26, 27). Using real-time PCR analysis, we found that the expression levels of these genes in pancreatic islets either exceed or are comparable to the levels in tissues where a functional role has previously been determined (Fig. S5). We also confirmed changes in mRNA expression of several up-

regulated genes that do not contain the *miR-375* motif, including tyrosine hydroxylase (*Th*) and neuronatin (*Nnat*) (Fig. 4*B*). Although the exact role of these genes in the pancreatic β cell is not known, it was shown that increased expression of neuronatin is associated with hyperglycemia-induced apoptosis (28, 29). Both genes appear to be indirectly regulated by *miR-375*, because reporter assays with vectors that harbor their 3′UTRs downstream of the luciferase gene did not result in decreased activity when co-expressed with *miR-375* (Fig. 4*D*). Together, these results provide evidence that many direct, as well as indirect, targets of *miR-375* contribute to the regulation of the β-cell composition of islets.

Discussion

Our results illustrate an essential role for *miR-375* in the establishment of normal pancreatic endocrine cell mass in the postnatal period and the maintenance of glucose homeostasis. The primary consequence resulting from the loss of *miR-375* is chronic hyperglycemia caused by a pancreatic α-cell defect, as evidenced by increased α-cell mass, increased glucagon release from isolated islets, elevated fasted and fed plasma glucagon levels, and the increase in downstream effects of glucagon, such as expression of genes regulating gluconeogenesis and hepatic glucose production. Of note, *375KO* mice in the fed state exhibit plasma glucagon levels that are comparable to fasted levels in wild-type mice, further emphasizing the chronic glucagon stimulus in these animals. The hyperglucagonemia in *375KO* mice compared with control littermates is most likely due to the increase in α-cell numbers and a defect in glucose sensing because exocytosis measurements in isolated α cells in response to direct depolarization was similar in wild-type and mutant mice. The hyperglycemic phenotype of *375KO* animals is unlikely due to the moderate (25%) decrease in β-cell mass because this reduction is usually insufficient to cause insulin deficiency and diabetes (30), and amounts of insulin secretion by isolated pancreatic islets from mutant and wild-type mice in response to various concentrations of glucose were similar. Furthermore, insulin levels in the fasted state and during a glucose challenge in *375KO* and wild-type littermates were similar, despite a reduced β-cell number in *375KO* mice, suggesting that insulin secretion per β cell is enhanced in *375KO* mice and that reduction of β-cell mass and increased secretion balance each other in mutant mice.

The mechanism by which loss of miR-375 function leads to a reduced β-cell mass is most likely mediated by the cluster of negative growth regulators that are directly regulated by miR-375 and are markedly up-regulated in *375KO* animals. The fact that the phenotype is more profound in mice with metabolic stress might indicate that miR-375 targets play a crucial role in β-cell compensation when metabolic demand is increased. The mechanism by which the α-cell number in *375KO* pancreata is increased is currently unknown. Two models can be proposed: miR-375 regulates specific target genes in α cells that are responsible for increased α-cell mass. Alternatively, the increase in α-cell number could be the result of a compensatory response to altered β-cell mass and function or to the chronic hyperglucagonemia, which in some models is associated with α-cell hyperplasia (31, 32).

Mice bearing a conditional deletion of *dicer*, an enzyme required for miRNA processing, during pancreas development exhibit defects in all pancreatic cell lineages, abnormal islet architecture, and a profound reduction in pancreatic β cells (8). Mutant *375KO* mice only partially mimic this phenotype, suggesting that *miR-375* alone is not responsible for the marked developmental defect in β-cell growth and differentiation and that other miRNAs, which are expressed in endocrine pancreatic precursor cells, must be responsible for the observed phenotype of the *Pdx-Cre*/*dicer* mice.

Last, it is interesting that *miR-375* plays a significant role in the hypertrophic growth response of pancreatic islets to metabolic stress. Expression levels of *miR-375* are aberrant in obese mice, indicating that they contribute to increased β-cell mass in insulin resistance. Ablation of *miR-375* expression in obese mice leads to a profound loss of β cells, metabolic decompensation, and premature death. Under these conditions, α-cell mass is not affected, suggesting that *miR-375* has a less prominent role in α cells, which are not under particular metabolic or cellular stress in hyperglycemic/insulin resistant conditions. Increasing evidence implicates miRNAs as an essential component mediating responses to cellular stress. For instance, tissue-enriched miRNAs in the heart, such as *miR-1*, *miR-208*, and *miR-133*, have been shown to regulate the hypertrophic proliferative activity in response to a variety of stresses, and *miR-126* affects survival after induction of a myocardial infarction (7, 12, 33). These observations from miRNA-knockout mice highlight the importance of small RNAs in cellular development, maintenance, and survival and reveal potential therapeutic targets for the treatment of disease.

Materials and Methods

Generation of *375KO* and *375/ob* Mice. The murine *miR-375* gene was deleted in *Sv129* ES cells by homologous recombination by using a targeting vector in which the entire pre-miRNA was deleted and replaced by a dsRed cDNA and Neo selection cassette (Fig. S1*A*). Targeted clones were identified by BstEII digests of genomic DNA and Southern blotting using the indicated 3′ probe. Approximately 10% of clones carried the targeted allele and 2 clones were used to generate chimeric animals that passed the mutant allele to offspring (Fig. S1*B*). Double *miR-375*$^{-/-}$, *Lep*$^{-/-}$ (*375/ob*) mice were generated by crossing double heterozygous mice and identified by PCR. Mice were housed in pathogen-free facilities in a 12-hr light/dark cycle and were backcrossed for 6 generations with C57BL/6 mice before characterization of animals. The dsRed transgene was not expressed. Unless stated, male animals were analyzed at 10 weeks of age.

Analysis of Metabolic Parameters. Blood glucose, insulin, glucagon, free fatty acids, and triglycerides in plasma were measured as described (16, 34). Vasoactive intestinal polypeptide (VIP), cocaine- and amphetamine-regulated transcript (CART), and secretin were measured by RIA (Phoenix Pharmaceuticals). The following hormones were measured by ELISA: glucagon-like peptide 1 (Linco), cortisol (US Biological), and growth hormone (Diagnostic Systems). Catecholamines were measured from plasma and tissues by HPLC. Individual animals were placed in metabolic cages to measure water consumption and urinary output (Columbus Instruments).

Glucose, Insulin, and Pyruvate Tolerance Tests; in Vivo Gluconeogenesis, and Hypothalamic–Pituitary–Adrenal Axis Stimulation Studies. Glucose tolerance tests were performed after mice were fasted overnight (16 hr) and injected i.p. with glucose (in saline) at 2 g/kg of body weight. Insulin tolerance tests were performed by injecting insulin i.p. (0.75 unit/kg of body weight), and measuring blood glucose before (time = 0) and 15, 30, and 60 min after injection. Pyruvate tolerance tests were also performed on mice in a random-fed state or after an overnight fast (16 hr) and injected i.p. with pyruvate (in saline) at 2 g/kg of body weight. In vivo gluconeogenesis studies were performed as previously described (35). Plasma corticosterone and ACTH were measured by RIA (Peninsula Laboratories and MP Biomedical, respectively).

Computational Analysis. The expression analysis of total RNA extracted from tissues of 10-week-old animals by using TRIzol reagents (Invitrogen) was performed by using Affymetrix mouse genome 430 2.0 arrays. Analysis of total RNA extracted from MIN6 cells infected with recombinant adenovirus expressing *miR-375* as described (13) was performed by using the Affymetrix mouse genome 430A array. Details on generation and analyses of data are found in *SI Methods*.

Northern Blotting, Quantitative PCR, Immunoblotting, and Luciferase Activity Measurements. Northern blotting, Western blotting, and luciferase assays were performed as previously described (13). Antibodies for Western blotting were obtained from several different sources: anti-gephyrin (Chemicon), anti-igsf4a/cadm (R & D Systems), anti-neuronatin (Abcam), anti-tyrosine hydroxylase (Abcam), and anti-HuD (gift of R. Darnell, The Rockefeller Uni-

versity, New York, NY). Primer sequences for real-time PCRs are available on request. miRNA quantitative PCR results were normalized to U6 levels, which were measured by using the ABI miRNA U6 assay kit (Applied Biosystems).

Immunohistochemistry, Islet Morphometry, and in Situ Hybridization. Immunohistochemistry was performed on at least 5 8-μm sections (at least 160 μm apart) prepared from paraffin-embedded pancreata of 3- and 10-week-old animals. Tissue sections were mounted with Vectashield with DAPI (Vector Laboratories) and analyzed by using a Leica DM5500 microscope, and the cross-sectional areas of pancreata and β cells (insulin-positive cells) were determined by using MetaMorph (version 7) software. Relative cross-sectional area of β cells was determined by quantification of the cross-sectional area occupied by β cells divided by the cross-sectional area of total tissue. β-Cell mass per pancreas was determined by the product of the relative cross-sectional area of β cells per total tissue and the pancreatic mass. Measurements were calculated by analyzing pancreata from at least 3 animals for each age and genotype. Cell quantification was based on counting nuclei of insulin-, glucagon-, or somatostatin-positive cells and data are represented as total cell number per pancreatic area. Ki-67- and BrdU-positive cells were counted from 1,500–2,000 insulin-positive cells per animal. Antibodies for immunofluorescence were obtained from several sources: anti-insulin and anti-glucagon (Linco), anti-somatostatin (Dako), anti-BrdU (Sigma), and anti-Ki-67 (Novocastra). BrdU incorporation and in situ hybridization were performed as described previously (9). Specific locked nucleic acid probes (Exiqon) were labeled by using terminal transferase and DIG-ddUTP (Roche).

ACKNOWLEDGMENTS. We thank J. Krutzfeldt, M. Spranger, C. Wolfrum, F. von Meyenn, M. Gstaiger, A. von Eckhardstein, A. Schaefer, R. Yi, and V. Horsley for advice and technical assistance. This work was supported in part by the Juvenile Diabetes Research Foundation, the National Institutes of Health, and the Wellcome Trust. M.N.P. was supported by a Ruth L. Kirschstein Fellowship. J.H. is partially supported by Schweizerische Nationalfonds Grant 3100A0-114001 to M.Z. M.T. was supported by a Juvenile Diabetes Research Foundation Post-Doctoral Fellowship.

1. Edlund H (2002) Pancreatic organogenesis—Developmental mechanisms and implications for therapy. *Nat Rev Genet* 3:524–532.
2. Gromada J, Franklin I, Wollheim CB (2007) alpha-Cells of the endocrine pancreas: 35 years of research but the enigma remains. *Endocr Rev* 28:84–116.
3. Shih DQ, et al. (2002) Profound defects in pancreatic beta-cell function in mice with combined heterozygous mutations in Pdx-1, Hnf-1alpha, and Hnf-3beta. *Proc Natl Acad Sci USA* 99:3818–3823.
4. Johnson JD, et al. (2003) Increased islet apoptosis in Pdx1$^{+/-}$ mice. *J Clin Invest* 111:1147–1160.
5. Ambros V (2004) The functions of animal microRNAs. *Nature* 431:350–355.
6. Bartel DP (2004) MicroRNAs: Genomics, biogenesis, mechanism, and function. *Cell* 116:281–297.
7. Zhao Y, et al. (2007) Dysregulation of cardiogenesis, cardiac conduction, and cell cycle in mice lacking miRNA-1-2. *Cell* 129:303–317.
8. Lynn FC, et al. (2007) MicroRNA expression is required for pancreatic islet cell genesis in the mouse. *Diabetes* 56:2938–2945.
9. Yi R, et al. (2006) Morphogenesis in skin is governed by discrete sets of differentially expressed microRNAs. *Nat Genet* 38:356–362.
10. Kloosterman WP, Lagendijk AK, Ketting RF, Moulton JD, Plasterk RH (2007) Targeted inhibition of miRNA maturation with morpholinos reveals a role for miR-375 in pancreatic islet development. *PLoS Biol* 5:e203.
11. Thai TH, et al. (2007) Regulation of the germinal center response by microRNA-155. *Science* 316:604–608.
12. van Rooij E, et al. (2007) Control of stress-dependent cardiac growth and gene expression by a MicroRNA. *Science* 316:575–579.
13. Poy MN, et al. (2004) A pancreatic islet-specific microRNA regulates insulin secretion. *Nature* 432:226–230.
14. Bock T, Pakkenberg B, Buschard K (2003) Increased islet volume but unchanged islet number in ob/ob mice. *Diabetes* 52:1716–1722.
15. Lim LP, et al. (2005) Microarray analysis shows that some microRNAs downregulate large numbers of target mRNAs. *Nature* 433:769–773.
16. Krutzfeldt J, et al. (2005) Silencing of microRNAs in vivo with 'antagomirs'. *Nature* 438:685–689.
17. Buckbinder L, et al. (1997) The p53 tumor suppressor targets a novel regulator of G protein signaling. *Proc Natl Acad Sci USA* 94:7868–7872.
18. Galbiati F, et al. (2001) Caveolin-1 expression negatively regulates cell cycle progression by inducing G_0/G_1 arrest via a p53/p21(WAF1/Cip1)-dependent mechanism. *Mol Biol Cell* 12:2229–2244.
19. Park BJ, et al. (2005) The haploinsufficient tumor suppressor p18 upregulates p53 via interactions with ATM/ATR. *Cell* 120:209–221.
20. Cohen AW, et al. (2003) Caveolin-1 null mice develop cardiac hypertrophy with hyperactivation of p42/44 MAP kinase in cardiac fibroblasts. *Am J Physiol* 284:C457–C474.
21. Kee BL (2005) Id3 induces growth arrest and caspase-2-dependent apoptosis in B lymphocyte progenitors. *J Immunol* 175:4518–4527.
22. Cheung EC, et al. (2006) Dissociating the dual roles of apoptosis-inducing factor in maintaining mitochondrial structure and apoptosis. *EMBO J* 25:4061–4073.
23. Kamal A, Datta K (2006) Upregulation of hyaluronan binding protein 1 (HABP1/p32/gC1qR) is associated with cisplatin induced apoptosis. *Apoptosis* 11:861–874.
24. Reyes JC, et al. (1998) Altered control of cellular proliferation in the absence of mammalian brahma (SNF2alpha). *EMBO J* 17:6979–6991.
25. Akamatsu W, et al. (2005) The RNA-binding protein HuD regulates neuronal cell identity and maturation. *Proc Natl Acad Sci USA* 102:4625–4630.
26. Kuramochi M, et al. (2001) TSLC1 is a tumor-suppressor gene in human non-small-cell lung cancer. *Nat Genet* 27:427–430.
27. Vaidyanathan G, et al. (2004) The Ras-related protein AGS1/RASD1 suppresses cell growth. *Oncogene* 23:5858–5863.
28. Borelli MI, Rubio M, Garcia ME, Flores LE, Gagliardino JJ (2003) Tyrosine hydroxylase activity in the endocrine pancreas: Changes induced by short-term dietary manipulation. *BMC Endocr Disord* 3:2.
29. Joe MK, et al. (2008) Crucial roles of neuronatin in insulin secretion and high glucose-induced apoptosis in pancreatic beta-cells. *Cell Signal* 20:907–915.
30. Bonner-Weir S, Trent DF, Weir GC (1983) Partial pancreatectomy in the rat and subsequent defect in glucose-induced insulin release. *J Clin Invest* 71:1544–1553.
31. Parker JC, Andrews KM, Allen MR, Stock JL, McNeish JD (2002) Glycemic control in mice with targeted disruption of the glucagon receptor gene. *Biochem Biophys Res Commun* 290:839–843.
32. Chen M, et al. (2005) Increased glucose tolerance and reduced adiposity in the absence of fasting hypoglycemia in mice with liver-specific Gs alpha deficiency. *J Clin Invest* 115:3217–3227.
33. Wang S, et al. (2008) The endothelial-specific microRNA miR-126 governs vascular integrity and angiogenesis. *Dev Cell* 15:261–271.
34. Kulkarni RN, et al. (2002) beta-cell-specific deletion of the Igf1 receptor leads to hyperinsulinemia and glucose intolerance but does not alter beta-cell mass. *Nat Genet* 31:111–115.
35. Leveille GA, Chakrabarty K (1968) In vivo and in vitro studies of gluconeogenesis in meal-fed and nibbling rats. *J Nutr* 96:397–402.